Study of alpha-radiation-induced deep levels in *p*-type silicon

M. Asghar, M. Zafar Iqbal, and N. Zafar
Semiconductor Physics Laboratory, Department of Physics, Quaid-i-Azam University, Islamabad, Pakistan

(Received 9 September 1992; accepted for publication 11 January 1993)

Deep levels introduced by 5.48 MeV alpha particles in *p*-type silicon have been studied using deep-level transient spectroscopy. The generation rates of these defects have been obtained up to a dose of 1.2×10^{11} α particles/cm^2. Detailed data have been obtained on the electrical characteristics of the two deep levels in the lower-half band gap at $E_v+0.21$ eV and $E_v+0.35$ eV and one level in the upper-half gap of silicon at $E_c-0.25$ eV introduced by irradiation. These characteristics include emission rate signatures, carrier capture cross sections, and their temperature dependence and deep-level concentrations. Detailed isochronal annealing measurements have been performed to obtain data on the annealing behavior of the deep-level defects and also to help identify these centers. Some interesting phenomena relating to temporal changes in our deep level spectra stimulated by minority carrier injection have been observed and discussed in the light of the available literature on radiation-induced defects in silicon.

I. INTRODUCTION

The study of radiation-induced defects in semiconductors constitutes an important area of research on semiconductors for fundamental reasons as well as from the point-of-view of device applications. For silicon, these studies, using high energy electron irradiation, have been principally motivated by the strong degradation effects on silicon solar cells caused by radiation during space use. γ rays and neutrons have also been used to study defects in silicon which are generally produced in electronic devices in nuclear radiation environment such as provided by nuclear reactors. Lately, α radiation from the packaging has been identified as the principal source of malfunction in the modern day silicon memory devices causing both soft[1] and hard[2] errors. Thus, alpha-particle-induced defects are a cause of primary concern for the in-use failure of these electronic applications of silicon devices, insofar as these defects can cause a permanent deterioration of the electrical characteristics of these devices even after low to moderate radiation doses. While a few studies of α-radiation-induced defects exist in the literature,[3–5] these have primarily focused on *n*-type material. Although Takeuchi *et al.*[2] have recently reported observation of some deep-level defects produced by alpha radiation in the upper-half band gap of *p*-type silicon, a detailed and comprehensive characterization of the defects in *p*-type material in both halves of the band gap is, in general, lacking in the literature.

We report here results of a study on *p*-type silicon exposed to α radiation. Deep-level transient spectroscopy (DLTS)[6] has been used to detect and provide a detailed characterization of the defect states introduced by radiation. Detailed data on the emission rates, capture cross sections, and line-shape characteristics have been obtained. Further insights have been provided by studying the production rates as a function of the radiation dose and high temperature annealing behavior of the radiation-induced deep-level defects.

II. MATERIAL AND EXPERIMENTAL DETAILS

We have used prefabricated n^+p junction diodes of silicon manufactured by RIFA AB of Sweden. The typical junction area of the diodes is ~0.35 mm^2 while the background doping concentration is $\sim1.8\times10^{15}$ cm^{-3} as determined from capacitance–voltage (C–V) measurements. Gallium rubbed with aluminum was used to provide the back ohmic contact and the device was mounted on a TO-5 header. Aluminum lead wire was bonded ultrasonically to provide the top contact. Each diode was routinely checked after bonding for good current–voltage (I–V) and (C–V) characteristics.

DLTS measurements were performed using a Metrimpex (Hungary) deep-level spectrometer model DSL-81 based on lock-in principle. The details of the instrument are described in Ref. 7. The samples on TO-5 headers were mounted in a variable-temperature cryostat consisting of two metallic blocks. The block holding the sample was fitted with a symmetrically placed second TO-5 header provided with a copper-constantan thermocouple to monitor the sample temperature. The sample could be cooled to 77 K by lowering the carefully shielded metallic block holding the sample and the thermocouple into a liquid-nitrogen Dewar and then heated, using a heater embedded in the metallic block. An automatic motor-driven variable capacitor was used to compensate for the background standing capacitance of the sample.

After routine assessment including current–voltage, capacitance–voltage, and DLTS measurements, the selected samples were exposed to α radiation from an ^{241}Am source emitting 5.48 MeV α rays, at room temperature. First DLTS measurements were always performed with a minimum loss of time ($\sim$10–15 min) after terminating irradiation to minimize any loss of information due to room-temperature annealing effects.

III. RESULTS

A. Deep level spectra

Figure 1 shows typical deep level emission spectra of our samples. Curves (a) represent majority- and minority-

 0021-8979/93/094240-08$06.00

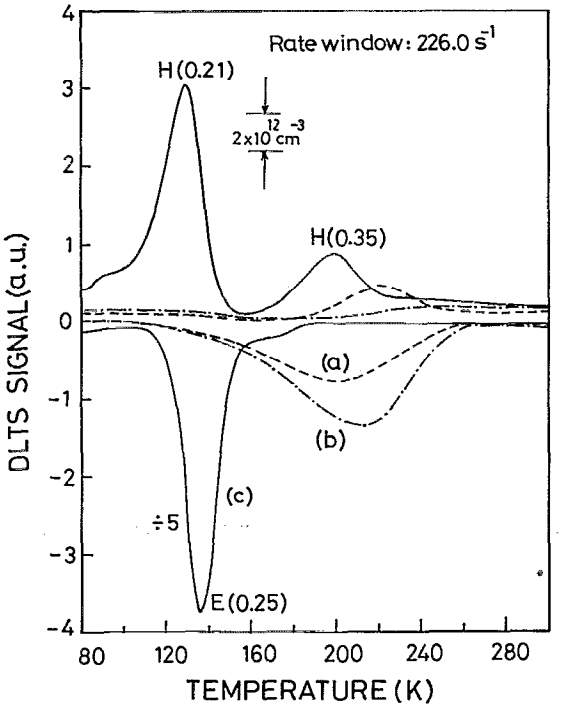

FIG. 1. DLTS spectra of (a) unirradiated virgin n^+p junction diodes (dashed), (b) preannealed unirradiated diodes (dot dashed), and (c) preannealed irradiated (dose: 1.2×10^{11} cm^{-2}) diodes (solid). The upper-half of the figure corresponds to hole emission and the lower part to electron emission; excitation pulse: -3.0—-0.5 V for majority carrier DLTS and 0–+1.0 V for injection DLTS. The marker represents the scale for the deep-level concentration.

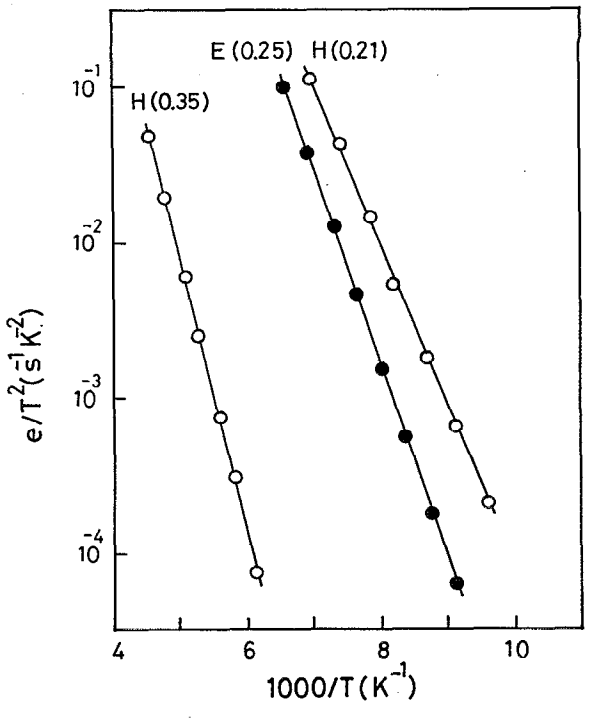

FIG. 2. Emission rate signatures of the α-induced deep levels in p-silicon observed immediately after irradiation.

carrier emission spectra obtained prior to irradiation. The spectra are clean except for one majority carrier (hole) emission peak and one minority carrier (electron) emission peak. These correspond to deep levels with energy positions $E_v+0.39$ eV and $E_c-0.23$ eV having concentrations $\sim8.0\times10^{11}$ cm^{-3} and $\geqslant2.4\times10^{12}$ cm^{-3}, respectively. These levels are obviously due to unintentional defects already present in our material. It was clear from irradiation of these virgin samples that we would face difficulty in obtaining unambiguous and accurate characterization of at least one of the radiation-induced hole levels due to a strong overlap with the preexisting $E_v+0.39$ eV level which forms a significantly high fraction of the radiation-induced peak height. In order to circumvent this difficulty, we gave a preannealing heat treatment in 20 min steps, similar to our subsequent isochronal annealing procedure discussed later, to some of our samples prior to irradiation. Heat treatment to ~300 °C led to almost complete anneal-out of the $E_v+0.39$ eV level, as shown in the DLTS scans Fig. 1(b). The $E_c-0.23$ eV preexisting electron level was still present in our samples after this preannealing procedure, but this does not interfere with our subsequent characterization of the radiation-induced electron level in view of its very small concentration as compared to that of the radiation-induced electron level.

These preannealed samples were used for irradiation studies in our subsequent work, although our preliminary results were obtained on the virgin samples to ascertain that the preannealing treatment did not disturb our later investigations. The typical DLTS scans for the preannealed irradiated samples are shown in Fig. 1(c). Two prominent hole emission peaks and a strong electron emission peak are clearly seen to arise as a result of α irradiation, in the first scans after irradiation.

B. Emission rates and activation energies

The emission rate signatures of all the radiation-induced deep levels observed are presented on the usual T^2-corrected Arrhenius plots in Fig. 2. The thermal activation energies determined from the slopes of these plots lead to the positions of the two hole levels as $E_v+0.21$ eV and $E_v+0.35$ eV while that of the electron level is found to be $E_c-0.25$ eV. These levels will henceforth be referred to as $H(0.21)$, $H(0.35)$, and $E(0.25)$, respectively. The extrapolated capture cross sections at $T=\infty$ obtained from the intercepts of the Arrhenius plots for these levels are listed in Table I.

C. Capture cross sections

Direct measurements of the hole capture cross sections of the radiation-induced levels were performed by investigating the peak height variation with excitation pulse width at a fixed temperature, in the usual way. This variation was, in general, found to be nonexponential which might be due to the contributions of more than one level latent in a given peak or due to the carrier tails in the edge of the depletion region even in the case of a single deep

TABLE I. Measured electrical parameters of α-particle-induced deep-level defects in p-silicon. $\sigma(\infty)$: thermal capture cross section for hole (p) or electron (n) obtained from the emission rate data. $\sigma(T)$: hole capture cross section directly measured at temperature T. N_T: typical deep-level concentration; for annealed-in defects, the annealing temperature after which N_T was measured is given in parentheses. η: production rate.

Deep level label	$\sigma(\infty)$ ($\times 10^{-15}$ cm^2)	$\sigma_p(T)$ ($\times 10^{-16}$ cm^2)	N_T ($\times 10^{12}$ cm^{-3})	η (cm^{-1})	T_{anneal} (°C)
$H(0.21)$	2.5(p)	0.12 2.90 (123 K)	13	~117	325 (-out)
$H(0.35)$	7.5(p)	0.08 2.40 (200 K)	5	~27.5	400 (-out)
$E(0.25)$	7.2(n)	···	>80	···	200 (-out)
$H(0.27)$ (injection-induced)	2.4(p)	···	0.2	···	···
$H(0.26)$	9.2(p)	3.00 (141 K)	8 (325 °C)	···	150 (-in) >400 (-out)
$H(0.20)$	49.7(p)	···	3 (300 °C)	···	270 (-in) >400(-out)

level. To isolate the contribution of this edge effect, we adopted the procedure followed by Meijer *et al.*[8] This consists in plotting the complete capture data as peak height versus logarithm of pulse width as shown in the inset of Fig. 3 for the hole level $H(0.21)$. The long-time part follows a straight line as predicted for the edge effect. The rest of the data points are then corrected by subtracting the edge region contribution obtained from this extrapolated line. The corrected data plotted in the main graph of Fig. 3 show the variation to follow a sum of two exponentials indicating the $H(0.21)$ peak to be composed of at least two deep levels. The capture cross sections obtained from the two exponentials are 1.2×10^{-17} cm^2 and 2.9×10^{-16} cm^2. The capture data on the $H(0.35)$ peak, are also found to correspond to two deep levels after edge-region correction using the same procedure. The corresponding capture cross sections are 8.5×10^{-18} cm^2 and 2.4×10^{-16} cm^2.

The temperature dependence of the hole capture cross section of the two hole levels was investigated from 108 to 123 K for the $H(0.21)$ level and from 187 to 224 K for the $H(0.35)$ level. No significant variation of the capture cross sections with temperature was found in both cases.

We also made an attempt to measure the hole capture cross section of the radiation-induced electron level at E_c -0.25 eV. This was achieved by filling the level with a wide (50 ms) electron injection pulse followed by a majority carrier (hole) "clear" pulse of successively increasing width. The decay of the DLTS peak height with increasing clear pulse width would provide a measure of the hole capture cross section of this deep level. Interestingly, the height of this peak hardly showed any significant decrease. This would appear to indicate that the hole capture cross section of this level was immeasurably small as compared to its electron capture cross section. However, this could alternatively be interpreted to imply a sharply decreasing depth profile beyond the built-in depletion region for the concentration of this deep level since our clear pulses essentially scan the region beyond this boundary. Clearly, it is impossible to differentiate between these two possibilities since it is not possible to measure the concentration profile of a minority-carrier emission peak using DLTS.

D. DLTS peak-shape analysis

In order to understand the capture data better, we investigated the line shapes of the observed DLTS peaks to look for any structures within the peaks. The theoretical peak profiles obtained from the expression given by Lang[9] for the lock-in principle of DLTS measurement, using the emission rate data of the main observed peak as the input, were compared with the observed peak profiles. Results of

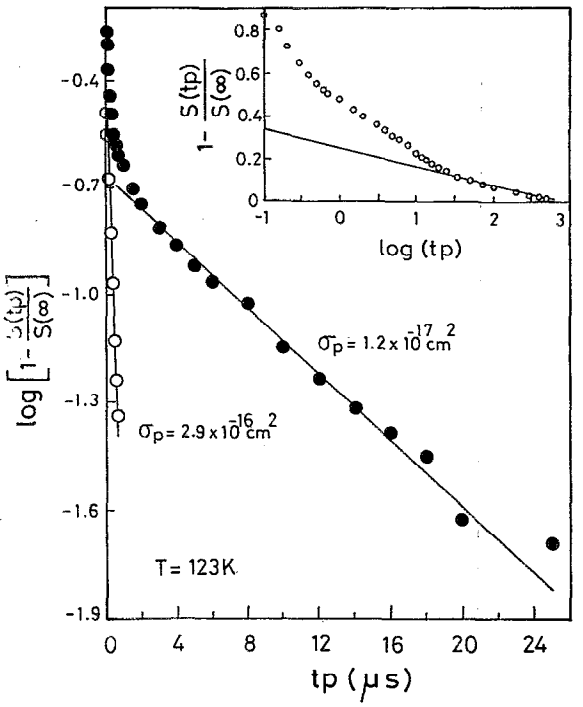

FIG. 3. Capture cross-section data of the hole level $H(0.21)$ at 123 K.

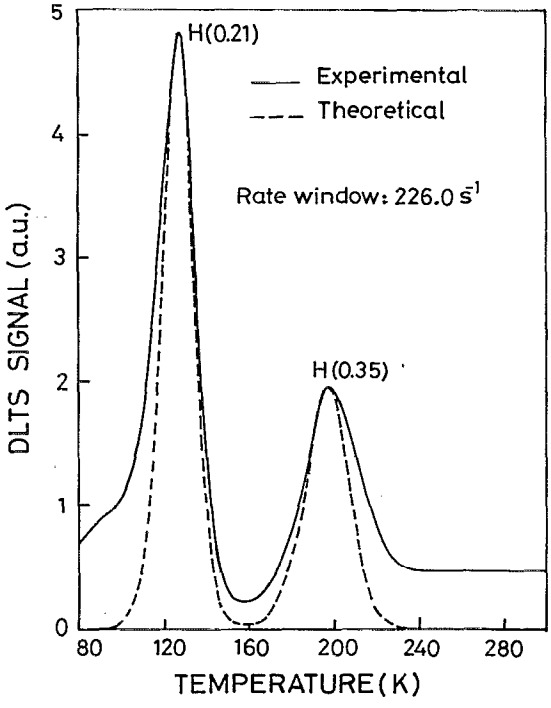

FIG. 4. DLTS peak shape analysis of the radiation-induced hole emission peaks. Solid curve: experimental spectrum, dashed curve: theoretical line fit for dominant peaks.

such an exercise are shown in Fig. 4 for a particular emission rate window. Neither of the two hole emission peaks shows a good fit to the theoretical line shape for a single deep level, indicating the presence of overlapping additional deep-level peaks. Our capture cross-section data fitting with double exponentials for both hole levels as discussed above are, thus, obviously consistent with this analysis of the peaks.

E. Production rates

The dose dependence of the generation of the observed deep levels was studied by exposing the samples to alpha radiation for increasing durations of time followed by DLTS scans. Care was exercised to check for any deterioration in the diode quality by performing reverse-bias I–V and C–V measurements on the samples after each irradiation step. The resulting deep level concentrations are plotted in Fig. 5 for the two hole levels $H(0.21)$ and $H(0.35)$. The production rates for the electron level could not be readily obtained in view of the expected incomplete filling of the minority carrier levels observed in injection DLTS. Besides, the data for this level may also suffer from inaccuracies due to possible changes in the injection characteristics of the diodes due to irradiation.

The production data for the levels $H(0.21)$ and $H(0.35)$ follow approximately linear increase with the radiation dose over the entire range of doses used (0–1.2 $\times 10^{11}$ cm^{-2}), as seen in Fig. 5. The production rates obtained from the slopes of the respective linear fits are found to be ~ 117 and ~ 27.5 cm^{-1}.

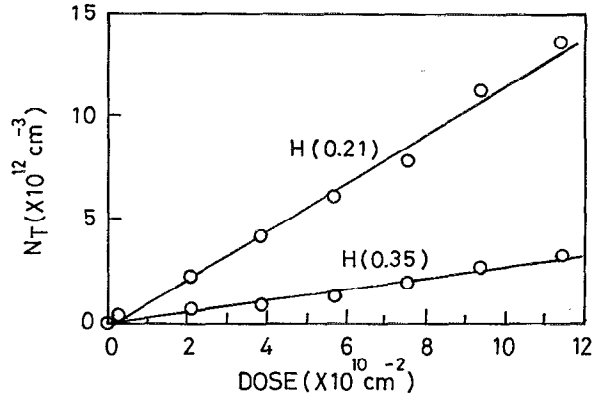

FIG. 5. Production rate data for the dominant radiation-induced hole levels.

During the dose dependence studies, we also observe a very broad peak appearing with a small height in the high temperature part of our spectrum at low radiation doses. The position of this feature, however, shifts towards lower temperatures as the dose is increased as shown in Fig. 6 and completely merges into the peak $H(0.35)$ at and beyond a dose of $\sim 7.6 \times 10^{10}$ cm^{-2}. This strange behavior is probably caused by a band of deep levels constituting this peak. Presumably the different components of this band have different production rates, thereby leading to a shift of the position of this feature. The energy position of these levels estimated from the peak temperature of this band is $\geqslant 0.4$ eV above the valence band edge.

F. Annealing characteristics

1. (Room-temperature) isothermal annealing induced by minority carrier injection

We have observed some interesting effects during our work whenever minority carrier injection pulses were applied to obtain minority carrier (electron) DLTS spectra of our samples after irradiation. These effects consist of (a) creation of a new majority carrier DLTS peak $H(0.27)$ corresponding to a deep level at $E_v + 0.27$ eV immediately after an injection scan (Fig. 7) accompanied by a slight decrease in the $H(0.21)$ peak; (b) significant enhancement in the peak height of the radiation-induced level $H(0.35)$ immediately after the injection scan; and (c) decay (anneal-out) of the new level $H(0.27)$ during storage of the samples at ambient temperatures, accompanied by a rise (anneal-in) of the radiation-induced peak corresponding to the level $H(0.35)$. The temporal variations of the concentrations of both these levels have been monitored during isothermal annealing at room temperature (18 °C) and are shown in Fig. 8 on a semilog plot. Both of these levels show similar annealing rates with a time constant of ~ 12 h at room temperature, indicating that probably the same kinetic process is involved in the room-temperature isothermal changes in the concentrations of these two levels.

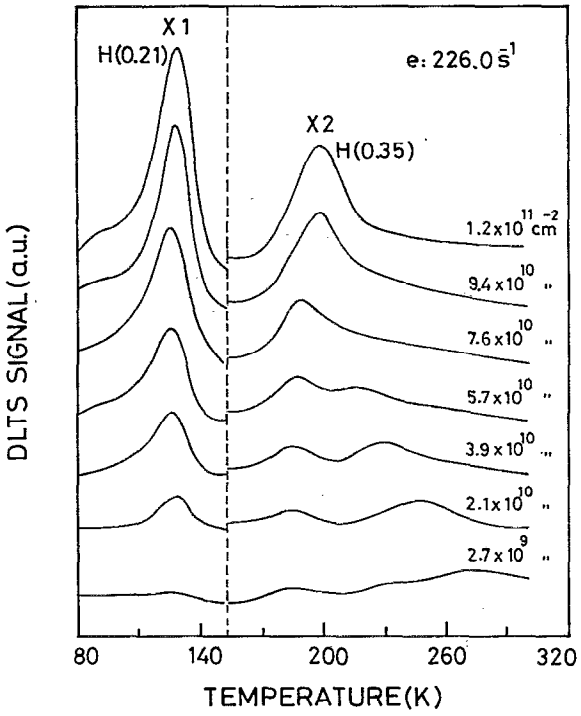

FIG. 6. Evolution of DLTS spectra with radiation dose. Note the small shifting peaks at the high temperature end.

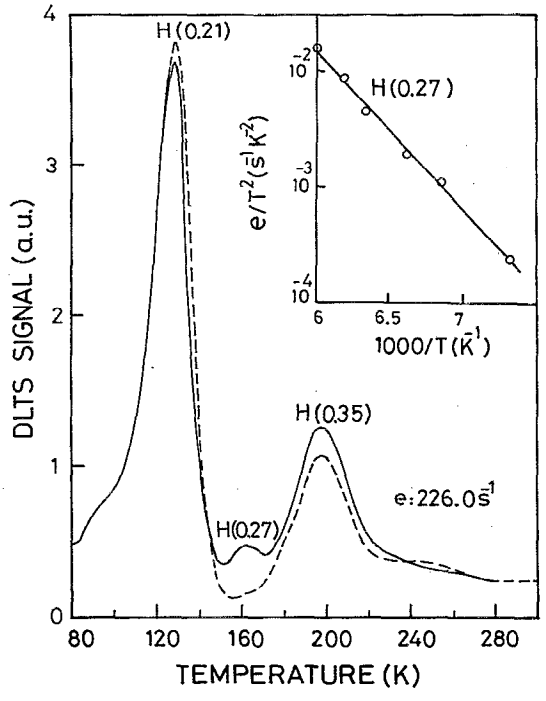

FIG. 7. Room-temperature injection-induced effects: majority carrier DLTS spectra immediately after irradiation (dashed) and after the first injection DLTS scan following irradiation (solid). Injection pulse used prior to the solid line spectrum: 0–+1.0 V; width 500 μs. Inset shows the Arrhenius plot of the emission rate data for $H(0.27)$ peak produced by injection.

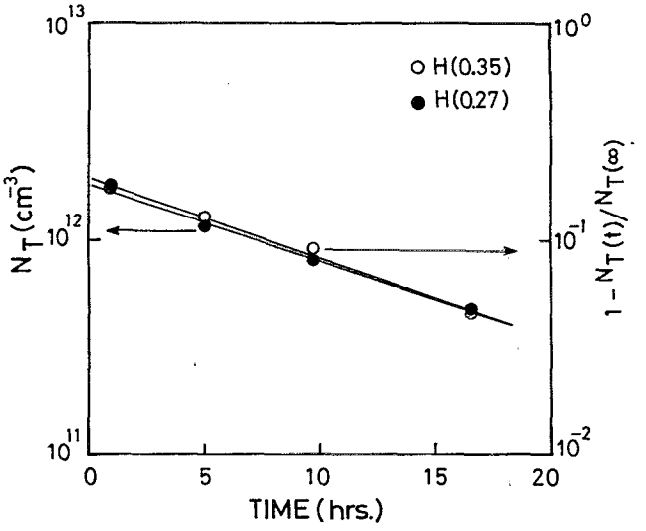

FIG. 8. Room-temperature (18 °C) isothermal anneal data for the growth and decay of $H(0.27)$ and $H(0.35)$ with time.

2. Isochronal annealing

The high temperature annealing behavior of the observed deep levels was characterized by isochronal (20 min) heat treatments of the irradiated samples at ~30 °C intervals followed by DLTS scans. Some of the resulting DLTS scans for majority carrier emission are presented in Fig. 9. The resulting isochronal annealing characteristics of the various levels are plotted in Fig. 10.

a. Anneal out of radiation-induced levels. The hole levels induced by radiation, $H(0.21)$ and $H(0.35)$, start declining gradually at ~50 °C, showing sharp drops followed by a complete anneal out close to 325 and 400 °C, respectively. The electron level $E(0.25)$, on the other hand, remains stable to ~150 °C whereafter its concentration shows a steep drop followed by a complete anneal out at ~200 °C.

b. Anneal in of new levels. Two new defects corresponding to deep levels at $E_v+0.2$ eV and $E_v+0.26$ eV are observed to be created at temperatures somewhat higher than ~270 and 150 °C, respectively, in our isochronal annealing studies of the irradiated samples as seen in Fig. 10. These levels are not observed during isochronal annealing of the unirradiated samples, indicating that these levels are created only during postirradiation annealing. The complete emission rate data for these levels are given in the inset of Fig. 9. The detailed annealing curves for these hole levels, $H(0.2)$ and $H(0.26)$, are presented in Fig. 10. The concentrations of these levels rise to a maximum at ~300 and ~325 °C, respectively, subsequently dropping to a low but finite ($\sim 2\times 10^{12}$ cm^{-3}) value at the highest annealing temperature used, i.e., 400 °C. It should be noted that the annealed-in defect $H(0.26)$ mentioned here is found to have a distinctly different emission rate signature as compared to the injection-induced $H(0.27)$ level described earlier.

In addition to these two levels, we also observe a broad peak appearing at ~260 K in our majority carrier emission

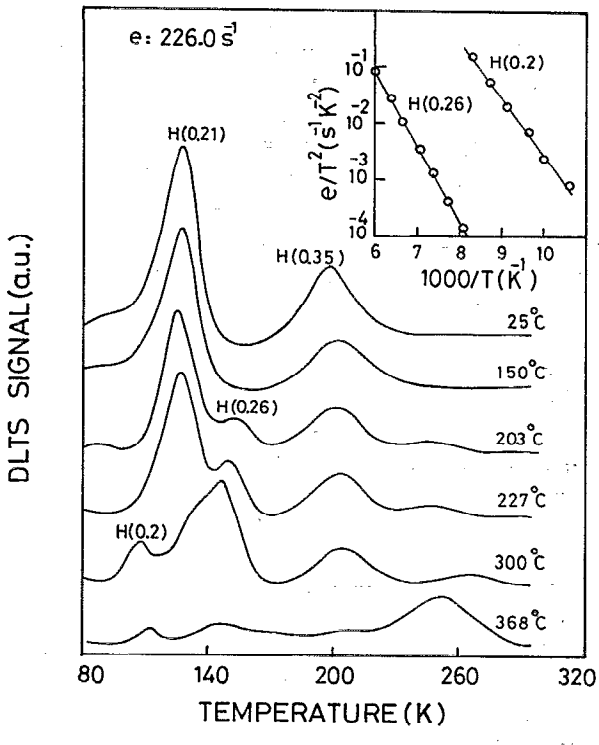

FIG. 9. DLTS spectra of irradiated samples as a function of annealing temperature. Note the small shifting peaks at the high temperature end. Inset shows the emission rate signatures of the annealed-in levels.

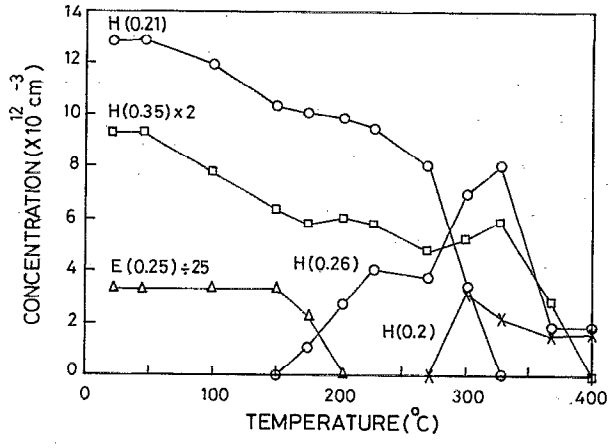

FIG. 10. Isochronal annealing characteristics of deep levels in irradiated *p*-silicon.

spectra beyond an annealing temperature of ~200 °C. This peak is, however, found to have an anomalous behavior insofar as its position shifts in an unsystematic manner with the annealing temperature as shown in Fig. 9. Presumably this feature consists of a band of more than one overlapping peaks which anneal-in and anneal-out at different temperatures thereby, leading to this rather strange behavior. This band of levels may correspond to the same band as seen in Fig. 6.

IV. DEFECT IDENTIFICATION AND DISCUSSION

A. 0.21 eV hole level

This level at $E_v+0.21$ eV has been previously observed in irradiation studies on *p*-type silicon, notably using electron beam irradiation.[10–13] The energy position, emission rate data, capture cross sections, and annealing data measured in this study lead to its probable identification as the (0/+) donor state of the divacancy (*V*–*V*) defect extensively reported in the literature.[12,13] The presence of a long-time tail in the capture data on this peak obviously points to the finite though small contribution of an unidentified deep level with a smaller capture cross section of $\sim 1.2 \times 10^{-17}$ cm^2 consistent with our line-shape analysis discussed above. The production rate of this level (117 cm^{-1}) for α particles is found to be at least two orders of magnitude larger than for 1 MeV electrons.[10,11]

B. 0.35 eV hole level

The production rate of this level (~ 27.5 cm^{-1}) is found to be about four times smaller than that of the *H*(0.21) divacancy level and $\sim 10^3$ times larger than that reported in the literature for irradiation by electrons.[10,11] It is interesting to note that the same deep level is found to have a production rate at least as high as 414 cm^{-1} in our α-irradiated *n*-silicon,[14] a point to be discussed in the latter part of this section.

At least three different defects with similar activation energies and emission rates have been identified in the literature. These are all related to the residual carbon impurity which has hitherto been proposed to form complexes directly with the radiation-produced primary defects or with secondary defects induced by radiation damage. These are the interstitial-carbon–interstitial-oxygen complex (C_i–O_i),[15] also called the C(3) center, the carbon–oxygen–vacancy complex (C–O–V),[11,13] also referred to as the *K* center and the interstitial–substitutional carbon complex (C_i–C_s).[12,16] The anneal-out temperature of the C_i–C_s center is, however, expected to be ~300 °C from the published work.[17] But we observe anneal out of the 0.35 eV DLTS peak at ~400 °C in agreement with the anneal-out characteristic of a level at similar energy ($E_v+0.38$ eV) observed by Mooney *et al.*[11] and by Lee *et al.*[13] ($E_v+0.33$ eV). Both of these reports suggested this level to originate from the (C–O–V) complex. However, identification with the C–O–V complex is, in general, not considered to be likely due to the absence of a correlation between the observed concentration of this level and that of the O–V complex (*A* center).[18] In fact, a detailed recent study, based on electron paramagnetic resonance (EPR) investigations combined with DLTS on electron-irradiated silicon by Song *et al.*,[19] has strongly ruled out the association of this level with the C_i–C_s center in favor of the C_i–O_i defect. This leaves the C_i–O_i complex as the most likely candidate for this level.

It is clear in view of the above discussion that the production rate of this deep level would be expected to strongly depend on the material and sample, since the in-

advertent carbon and oxygen contamination could vary with the material as well as with device processing and it would, in general, be impossible to specify the amount of these impurities in the finished junction devices with certainty. Further, these impurities can also form complexes with the different deliberate dopants in n- and p-type materials leaving very different amounts for the formation of the $E_v+0.35$ eV deep level during irradiation. It is, therefore, hardly surprising that we have observed more than an order of magnitude higher production rate for this level in our α-irradiation work on n-type silicon.[14]

C. 0.25 eV electron level

A comparison of the activation energy and the emission rate signature of this level with published data seems to point to V–V ($--/-$) state of the divacancy defect as one possible candidate for this defect. However, the divacancy is known to anneal out at $\sim$300 °C in all the published electron irradiation studies[10,16] as well as in our alpha-irradiation work on n-type silicon,[14] whereas we find the $E_c-0.25$ eV level to anneal out at $\sim$200 °C. Kimerling[12] has also observed an electron level ($E_c-0.26$ eV) in his p-type samples with an emission rate signature identical to that of the V–V ($--/-$) level of the divacancy observed in his n-type samples. The anneal-out temperature of this electron level in his p-type samples was, however, found to be $\sim$150 °C. Mooney *et al.*[11] have observed a level at $E_c-0.27$ eV in their electron irradiated p-type samples with an anneal-out temperature (200 °C) almost the same as in our case. Both Kimerling[12] and Mooney *et al.*[11] also report the emergence of a hole level at $E_v+0.30$ eV accompanying the anneal out of their electron level mentioned above. This observation is strikingly similar to ours. The anneal-out temperature ($\sim$400 °C) of the new level $H(0.26)$, emerging after the disappearance of the $E(0.25)$ level in our study, also agrees with the observations of Kimerling[12] and Mooney *et al.*[11] Following Mooney *et al.*[11] we interpret our $E(0.25)$ level to be probably associated with an interstitial–boron–interstitial-oxygen (B_i–O_i) complex which transforms to a vacancy–oxygen–boron (V–O–B) complex upon annealing, giving rise to the $H(0.26)$ level in our study.

D. Injection-induced level $H(0.27)$

This level is found to have emission rate signature very close to that of the $E_v+0.29$ eV level seen by Walker and Sah,[10] which has subsequently been observed in other studies[11,13,20] on electron irradiated silicon as well and has been generally attributed to the interstitial carbon (C_i) defect. It has also been reported to anneal out at or around room temperature although different anneal out times are found by different authors which vary from $\sim$1 h,[13] to a few days.[11] But all these reports differ in an important aspect from our observation, i.e., while in these studies this level is observed immediately after irradiation, we fail to observe it in our DLTS scan immediately after irradiation or even after $\sim$72 h of storage time at room temperature. In our case, this level is observed only after a minority carrier injection DLTS scan is performed, showing clearly that the creation of this defect is somehow associated with minority carrier injection. The fact that simultaneously with the generation of $H(0.27)$ an enhancement of the carbon-related peak $H(0.35)$ is observed which subsequently grows further during storage as the $H(0.27)$ peak decays, seems to strengthen the possibility that the $H(0.27)$ level is associated with the C_i defect. The similar time constants observed for the room temperature changes in the concentration of these levels further strengthen this interpretation. However, detailed further work is needed to understand why it is not observed without minority carrier injection in our case. Such work is also expected to shed light on the detailed mechanism of the recombination-enhanced defect reaction which is apparently responsible for the creation of this defect. Such investigations are planned to be undertaken in future. But due to the observed relationship between the $H(0.27)$ level and the $H(0.35)$ level, their complementary decay and growth during room-temperature isothermal annealing and the similarity of observed emission signature of $H(0.27)$ with that reported for the C_i defect,[10] we are inclined to conclude, at present, that our $H(0.27)$ level is probably associated with interstitial carbon.

V. CONCLUSIONS

In conclusion, we have reported a detailed study on the alpha-radiation induced defects in p-type silicon for the first time, to the best of our knowledge. This study shows that the $H(0.21)$V–V ($0/+$) defect and the $H(0.35)$ deep level probably associated with the C_i–O_i complex, are the dominant deep-level defects produced in the lower-half band gap of silicon. A prominent electron level $E(0.25)$ probably due to B_i–O_i complex, but deceptively similar to the V–V($--/-$) defect in some respects, is created in the upper-half gap of the material. These levels are commonly observed in silicon irradiated with electrons and other types of radiation. Useful detailed data on the properties of these defects have been provided. We have additionally observed interesting deep-level generation and subsequent isothermal annealing phenomena in our alpha-irradiated samples associated with minority carrier injection. The detailed nature and mechanisms of these phenomena would form the subject of our continuing investigations. We also observe a band of hole levels in the high temperature part of our DLTS spectra with estimated activation energy greater than 0.4 eV which may be associated with extended defects produced by alpha radiation.

ACKNOWLEDGMENTS

It is a pleasure to thank Dr. Andrej Litwin of Rifa AB, Sweden for some of the samples. Dr. N. Baber is thanked for a critical reading of the manuscript.

[1] T. C. May and M. H. Woods, IEEE Trans. Electron Devices **ED-26**, 2 (1979).
[2] K. Takeuchi, K. Shimohigashi, H. Kozuka, T. Toyabe, K. Itoh, and H. Kurosawa, IEEE Trans. Electron Devices **ED-37**, 730 (1990).

[3]L. S. Berman, A. D. Remenyuk, and V. B. Shuman, Sov. Phys. Semicond. **15**, 665 (1981).
[4]V. I. Gubskaya, P. V. Kuchinskii, V. M. Lomako, and A. P. Petrunin, Sov. Phys. Semicond. **15**, 243 (1979).
[5]H. Indusekhar, V. Kumar, and D. Sengupta, Phys. Status Solidi A **93**, 645 (1986).
[6]D. V. Lang, J. Appl. Phys. **45**, 3023 (1974).
[7]G. Ferenczi and J. Kiss, Acta Phys. Acad. Sci. Hung. **50**, 285 (1981).
[8]E. Meijer, H. G. Grimmeiss, and L. A. Ledebo, J. Appl. Phys. **55**, 4266 (1984).
[9]D. V. Lang, in *Thermally Stimulated Relaxation in Solids*, edited by P. Braunlich (Springer, New York, 1979), p. 93.
[10]J. W. Walker and C. T. Sah, Phys. Rev. B **7**, 4587 (1973).
[11]P. M. Mooney, L. J. Cheng, M. Süli, J. D. Gerson, and J. W. Corbett, Phys. Rev. B **15**, 3836 (1977).
[12]L. C. Kimerling, *International Conference on Radiation Effects in Semiconductors*, edited by N. B. Urli and J. W. Corbett, *Dubrovnik, 1976*, Inst. Phys. Ser. No. 31 (IOP, Bristol, 1977), p. 221.
[13]Y. H. Lee, K. L. Wang, A. Jaworowski, P. M. Mooney, L. J. Cheng, and J. W. Corbett, Phys. Status Solidi A **57**, 697 (1980).
[14]M. Ashgar, M. Zafar Iqbal, and N. Zafar, J. Appl. Phys. **73**, 3698 (1993).
[15]J. M. Trombetta and G. D. Watkins, Appl. Phys. Lett. **51**, 1103 (1987).
[16]L. C. Kimerling, IEEE Trans. Nucl. Sci. **NS-23**, 1497 (1976).
[17]K. L. Brower, Phys. Rev. B **14**, 872 (1976).
[18]C. A. Londos, Semicond. Sci. Technol. **5**, 645 (1990).
[19]L. W. Song, X. D. Zhan, B. W. Benson, and G. D. Watkins, Phys. Rev. B **42**, 5765 (1990).
[20]C. A. Londos, Phys. Status Solidi A **92**, 609 (1985).